

# Design of A Portable Optical Fiber-Based Localized Surface Plasmon Resonance (LSPR) for In-Situ Biosensing

N.S.Susan Mousavi<sup>1,2</sup>, F. Moghaddasi<sup>1</sup>, P. Venugopalan<sup>3</sup>, A.Dabirian<sup>1</sup>, S.Kumar<sup>2,3</sup>

<sup>1</sup> School of Physics, Institute for Research in Fundamental Sciences(IPM), Tehran, Iran

<sup>2</sup> Department of Mechanical Engineering, New York University, Brooklyn, USA

<sup>3</sup> New York University, Saadiyat Island, Abu Dhabi, UAE

## Introduction

➤ Since late 1980s, different methods have been developed for fiber-based biosensing. *Lab-on-fiber* technology in label-free and real-time *in-situ* monitoring for biomedical and clinical fields has been used for:

- *In vivo* (in the living organism) or *in vitro* (within the glass, laboratory use) applications
- Noninvasive, contacting (skin surface), minimally invasive (indwelling), or invasive (implantable) applications

➤ **Plasmonic Biosensing** has been enhanced by integration of optical fibers with metallic nanostructures.

➤ **Localized surface plasmon resonance**-based (LSPR) biosensors has further advanced the field with the progress in nanofabrication and nanochemistry.

➤ Considering easy preparation, biocompatibility, inertness, and intense light emissions, gold (Au) nanoparticles have advantages over other materials such as silver (Ag).

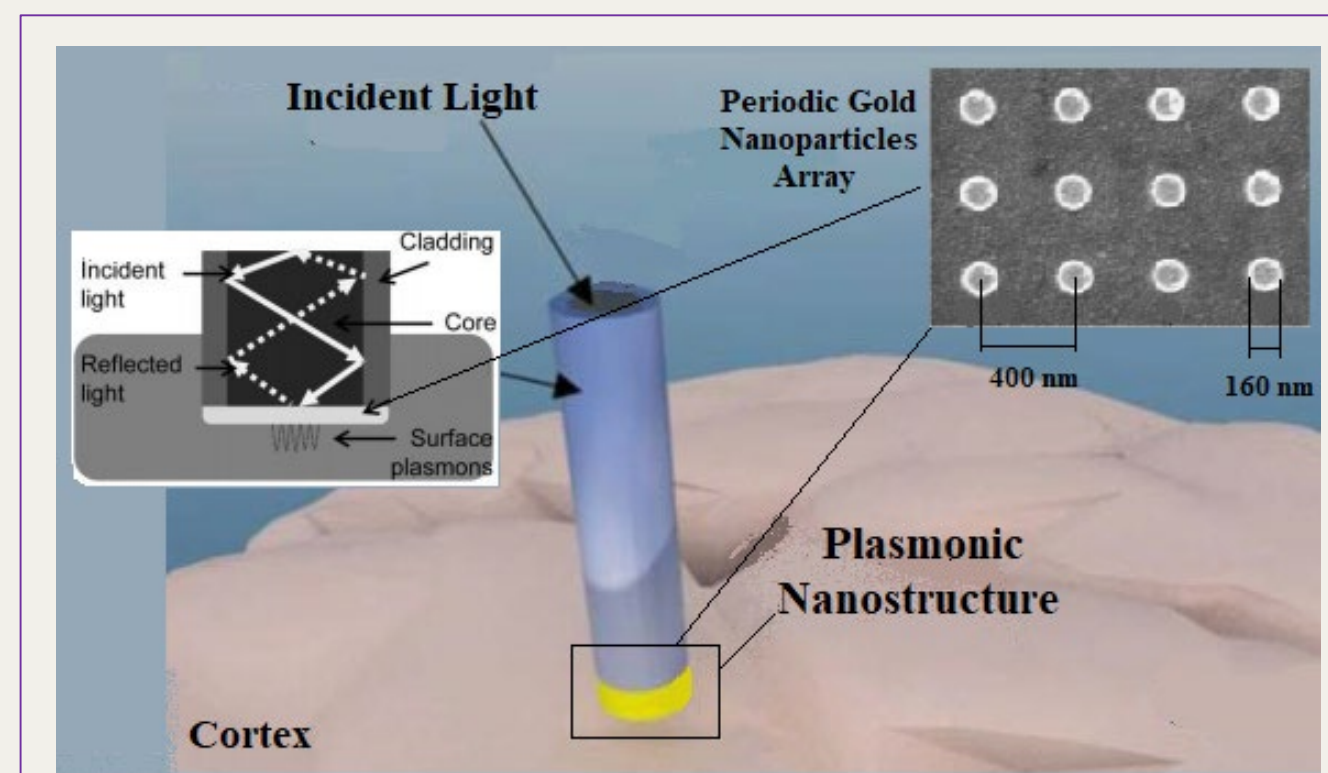
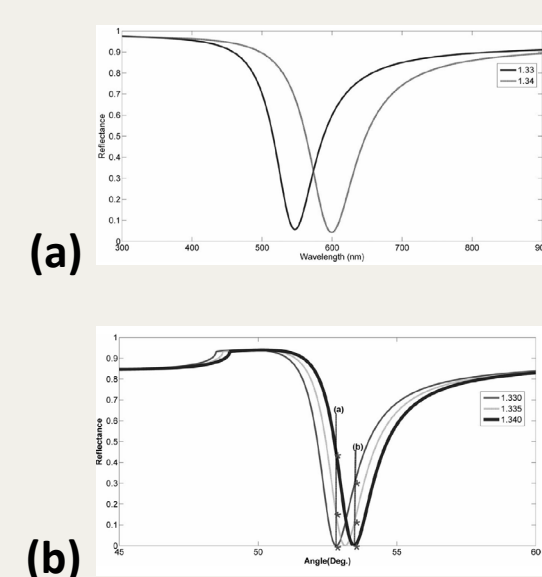


**Fig.1** Schematic of end face coated fiber-based LSPR biosensor Ref [2,3].

### Excitation of Surface Plasmon Resonances

$$\sqrt{\epsilon_p} \sin \theta_{res} = \left[ \frac{\epsilon_m \epsilon_s}{\epsilon_m + \epsilon_s} \right]^{1/2}$$

$\epsilon_p, \epsilon_m, \epsilon_s$  are, respectively, glass, metal, and dielectric constant Ref [1]



### Sensitivity

(a) Sensitivity of wavelength interrogation

$$S_\lambda (\text{nm}/\text{RIU}) = \Delta \lambda_{\text{resonance}} / \Delta n_a$$

(b) Sensitivity of amplitude interrogation

$$S_A (\lambda) \text{ RIU}^{-1} = -(\partial a(\lambda, n_a) / \partial n_a) / a(\lambda, n_a)$$

Nominator is the change in amplitude (i.e.  $\Delta a$ ) as RI changes, denominator is amplitude value (a) at wavelength and RI of medium ( $n_a$ ).

## Results (Continued)

### Effects of Shape and Material on Absorption spectra

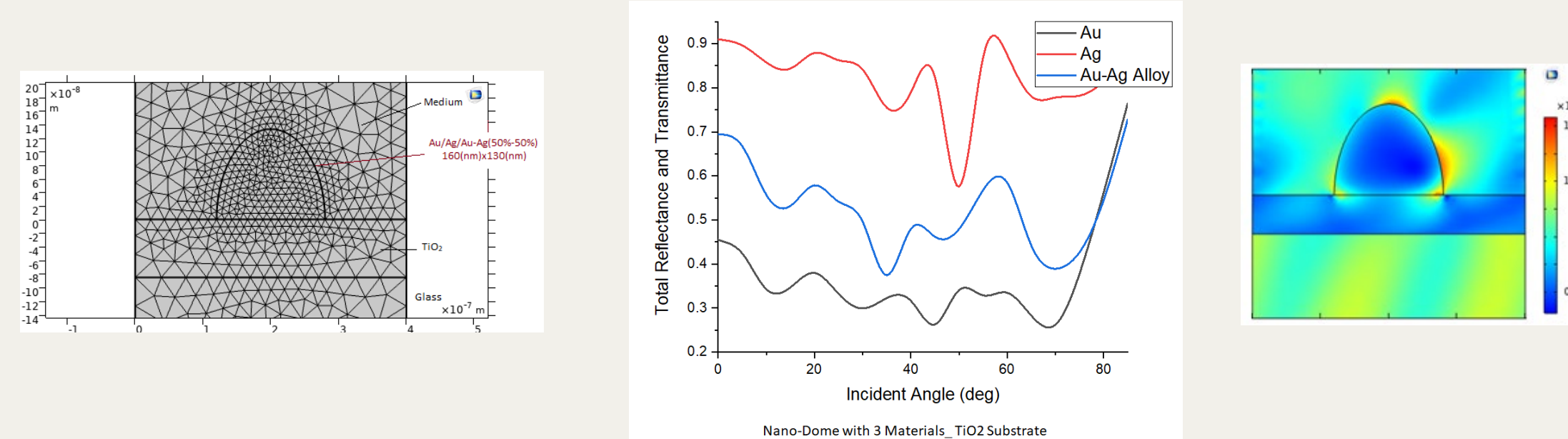


**Fig.6** The nanodome of size 160[nm]x130[nm] on TiO<sub>2</sub>-coated glass substrate has been considered (see the mesh). For the plasmonic nanostructure, Au, Ag, and alloy of Au-Ag (50%-50%) have been used. Plot of the total transmittance and reflectance for the 3 materials shows better performance for the gold nanostructure (middle). Localized resonance coupling at the selected wavelength of 560 (nm) and RI=1.38,  $\alpha=65$  [deg] for Au nanoparticle can be seen (right).

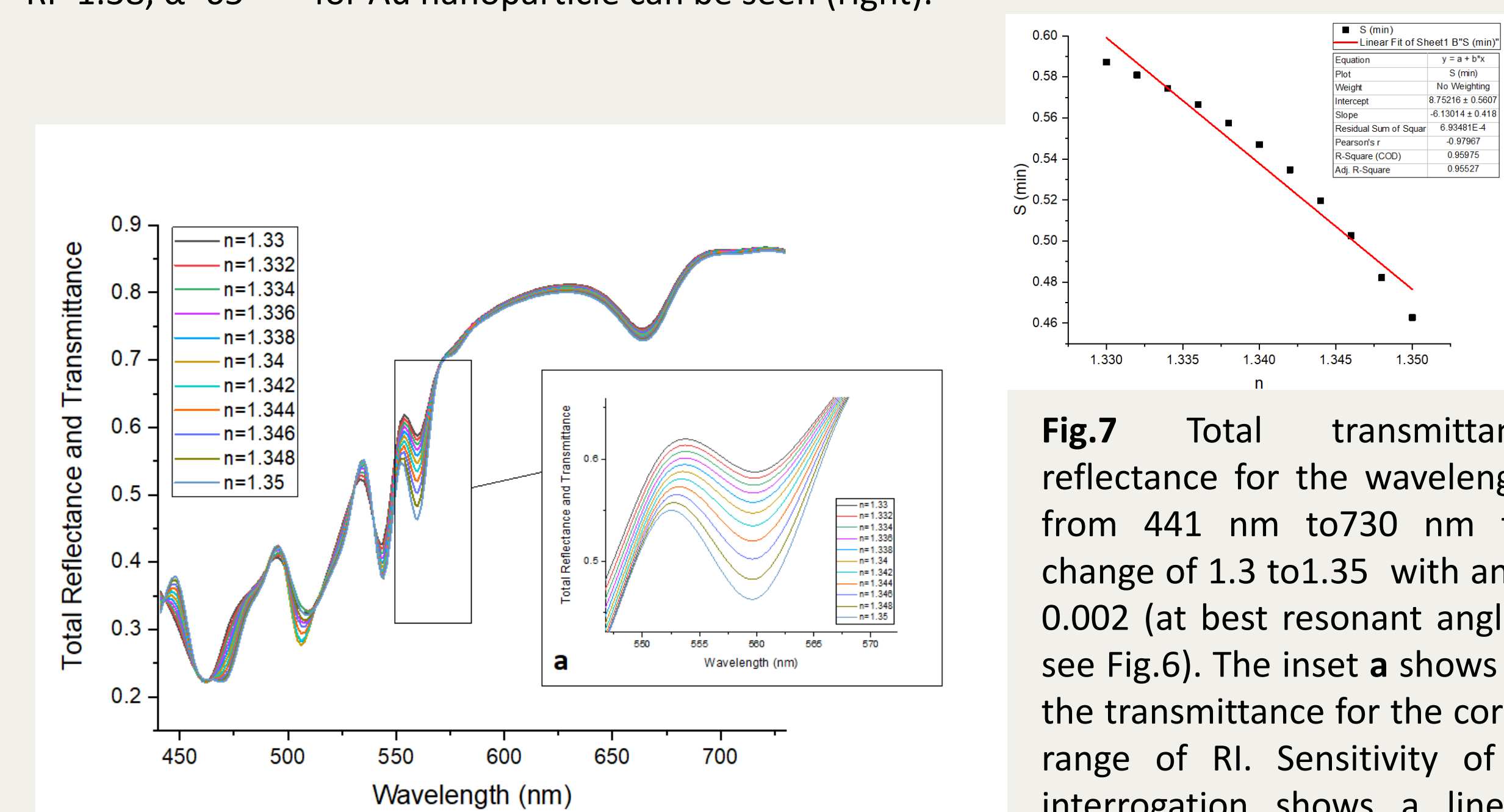


**Fig.7** Total transmittance and reflectance for the wavelength ranging from 441 nm to 730 nm for the RI change of 1.3 to 1.35 with an increment 0.002 (at best resonant angle  $\alpha=65$  [deg], see Fig.6). The inset shows the shift in the transmittance for the corresponding range of RI. Sensitivity of amplitude interrogation shows a linear pattern with RI change (top right).

## Method

### Using FDTD, the structure in Ref[1] is modeled:

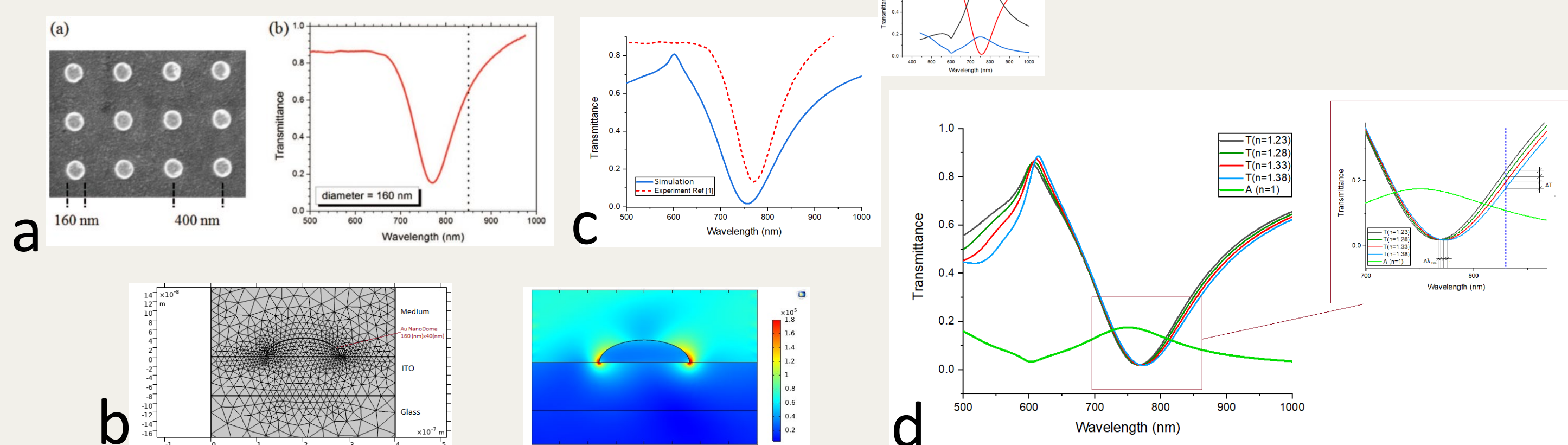


**Fig2.** Plasmonic templates (Au nanodome of size 160[nm]x40[nm]) fabricated on indium tin oxide (ITO)-coated glass substrate using EBL patterning and transmittance spectrum in air and normal incident ( $\alpha=0$ ) Ref[1] (a). Mesh structure of the model for FDTD simulation (b). Transmittance spectrum at normal incident from simulation showing good agreement with the experimental curve from Ref[1] (c). TM electric field at the reported resonance condition ( $\lambda=785$  nm) shows strong coupling on the corners but weak coupling on top of Au nanodome (b right inset). Simulated transmission spectra for 4 different refractive indexes (RI), and their corresponding shifted wavelength, and amplitude (see d and the inset). For ease of comparison, total absorbance for air are also plotted in (d) showing weak absorbance at the reported resonance point.

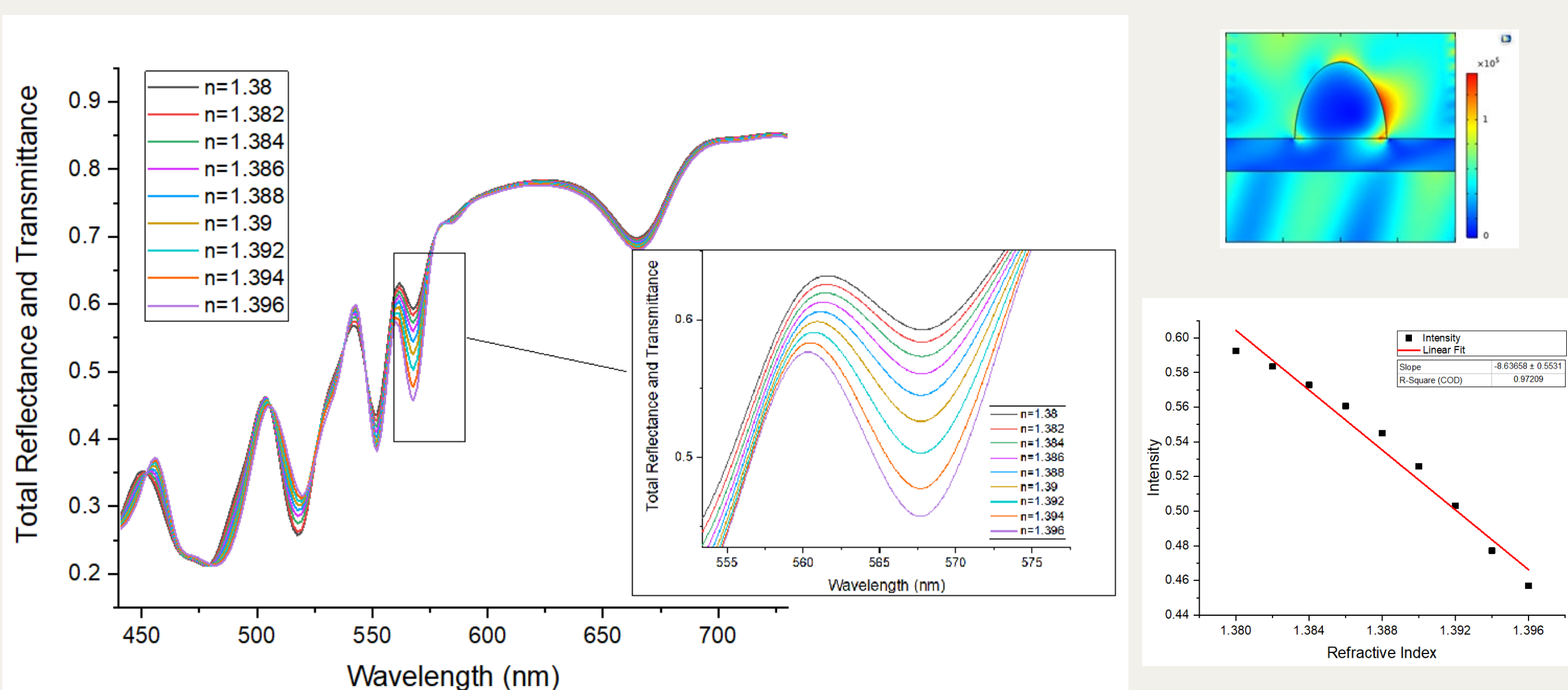


**Fig. 8** Curves of total transmittance and reflectance for gold nanodome structure. RI varies from 1.38 to 1.396 (increment of 0.002) (left). The inset shows a close view of the localized resonance condition. The shifts in the transmittance is linear with respect to the RI (bottom right). A selected localized excitation of SPP is shown on TM electric field (top right).

## Results

### Investigation of the enhancement of the surface coupling

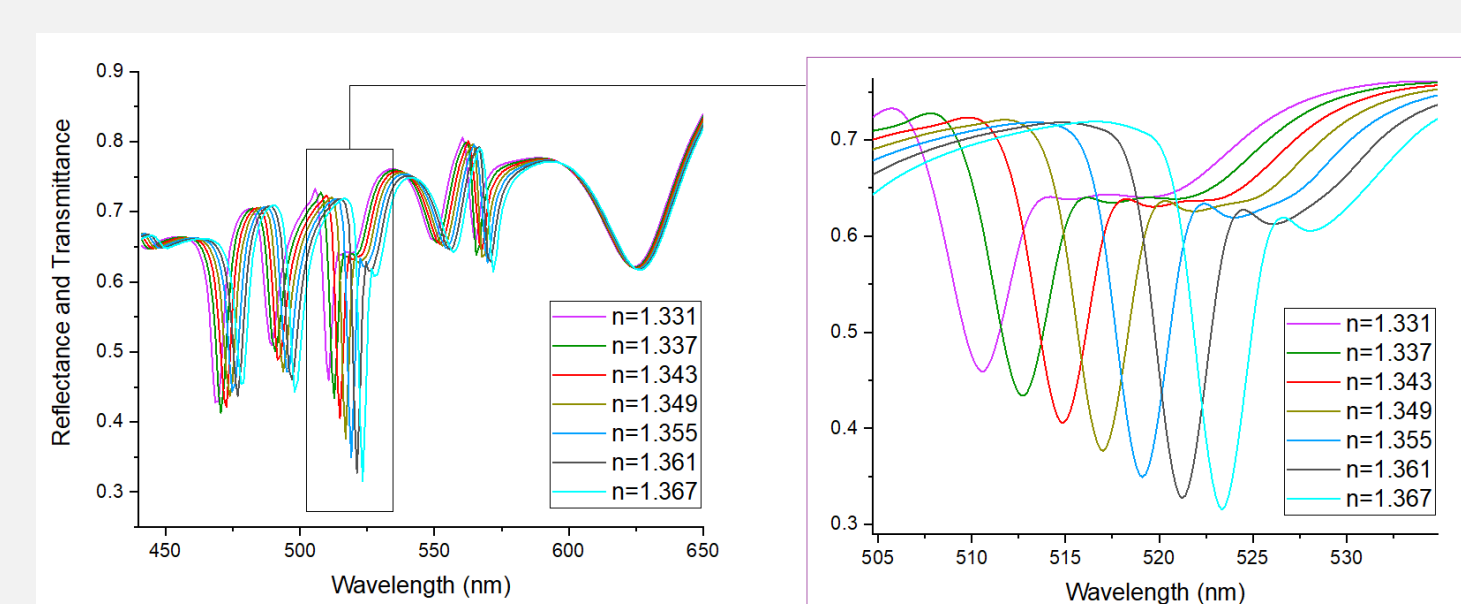


**Fig.3** Simulation has been extended for smaller wavelength range. Multiple dips (representing peaks in absorbance) are observed in the plot of total transmittance and reflectance for  $\alpha=70$  [deg]. Matching with TM electric field view, a window of wavelength where strong surface coupling is observed (due to the bragg diffractive mode at the medium-nano dome interface), has been selected. Corresponding curves can be seen (left inset).

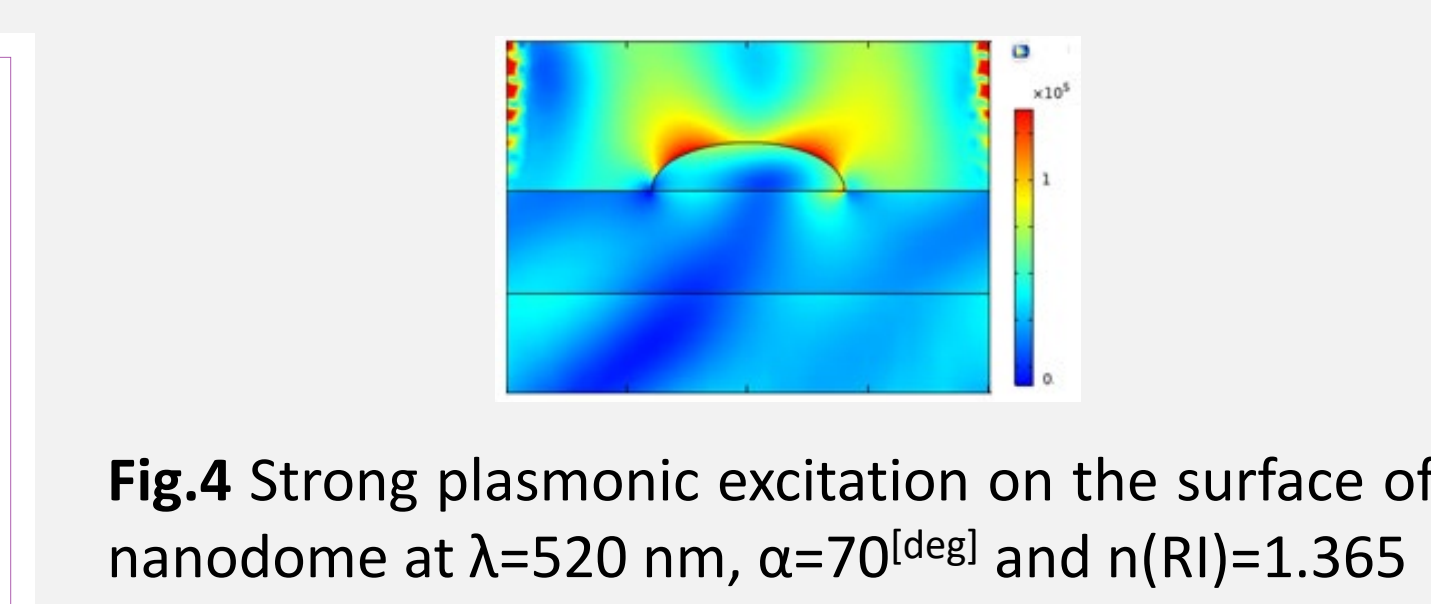


**Fig.4** Strong plasmonic excitation on the surface of nanodome at  $\lambda=520$  nm,  $\alpha=70$  [deg] and  $n(\text{RI})=1.365$

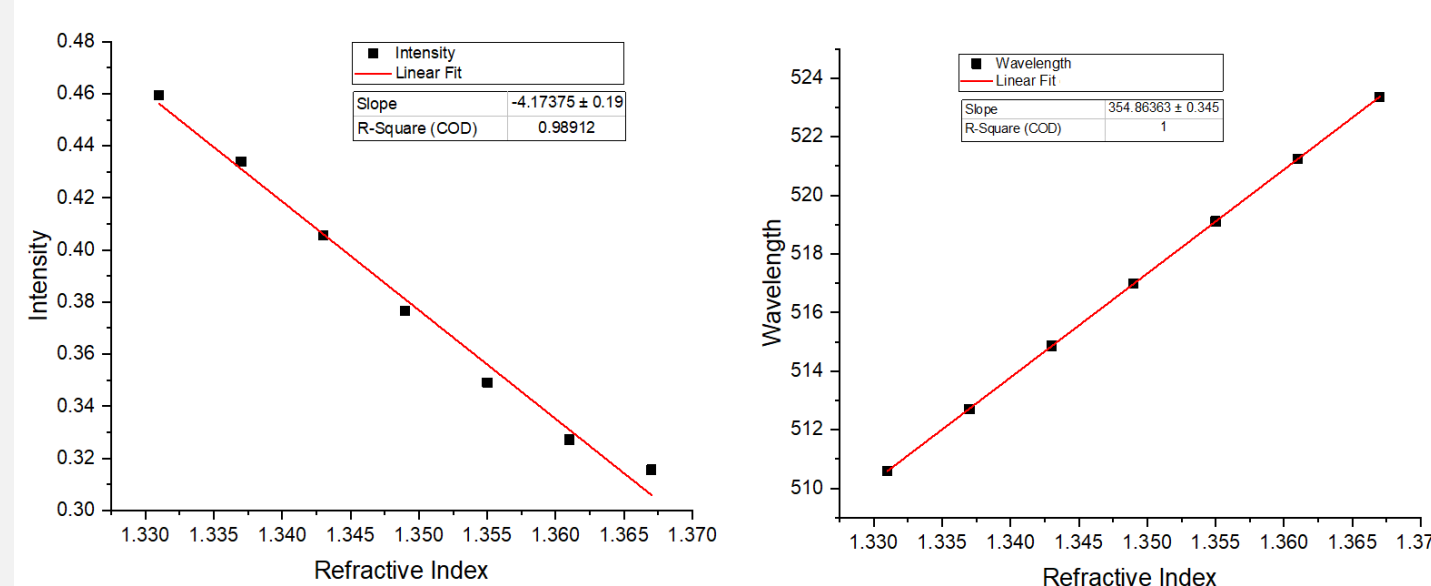


**Fig.5** Shift in intensity (left)/ resonance wavelength (right) vs. refractive index (increment=0.005). Linear response is observed in both.

## Conclusion and Future Work

- A periodic plasmonic nanostructure that has experimentally been used for recording brain cell activity is modeled for a simulation-based analysis.
- The results of the simulation have shown a good agreement with the experimental findings (note that small deviation is due to the normalized experimental results with respect to the unpatterned substrate).
- In the platform of lab-on-fiber, a similar structure has been considered at the end face of an optical fiber.
- The effects of shape and material of nanodome, and substrate materials have been investigated to further enhance the sensitivity of the biosensor to the change of Refractive index (RI) of the medium.
- The results show the localized excitation of the surface plasmon polaritons on the metal nanoparticles.
- The responses are found to be linear for the reported RI ranges.
- We further investigate resolution of the biosensor in order for use in recording high temporal signals of action potentials.

## References

1. Gupta, B, Srivastava, S. K., Verma, R. (2015). Fiber optic sensors based on plasmonics. World scientific.
2. Zhang, J., Atay, T., & Nurmikko, A. V. (2009). Optical detection of brain cell activity using plasmonic gold nanoparticles. Nano Letters, 9(2), 519-5242.
3. Kim, S.A. Kim, S.J., Moon H. & Jun, S.B. (2012). In vivo optical neural recording using fiber-based surface plasmon resonance. Optics Letters. 37 (4) 614.